Journal of Thrombosis and Haemostasis, **15**: 1655–1667 DOI: 10.1111/jth.13745

ORIGINAL ARTICLE

Intracellular origin and ultrastructure of platelet-derived microparticles

A. A. PONOMAREVA,*† T. A. NEVZOROVA,* E. R. MORDAKHANOVA,* I. A. ANDRIANOVA,* L. RAUOVA,‡§ R. I. LITVINOV§ and J. W. WEISEL§

**Institute of Fundamental Medicine and Biology, Kazan Federal University; †Kazan Institute of Biochemistry and Biophysics, Russian Academy of Sciences, Kazan, Russia Federation; ‡The Children's Hospital of Philadelphia; and §University of Pennsylvania School of Medicine, Philadelphia, PA, USA*

To cite this article: Ponomareva AA, Nevzorova TA, Mordakhanova ER, Andrianova IA, Rauova L, Litvinov RI, Weisel JW. Intracellular origin and ultrastructure of platelet-derived microparticles. *J Thromb Haemost* 2017; **15**: 1655–67.

Essentials

- Platelet microparticles play a major role in pathologies, including hemostasis and thrombosis.
- Platelet microparticles have been analyzed and classified based on their ultrastructure.
- The structure and intracellular origin of microparticles depend on the cell-activating stimulus.
- Thrombin-treated platelets fall apart and form microparticles that contain cellular organelles.

Summary. *Background:* Platelet-derived microparticles comprise the major population of circulating blood microparticles that play an important role in hemostasis and thrombosis. Despite numerous studies on the (patho)-physiological roles of platelet-derived microparticles, mechanisms of their formation and structural details remain largely unknown. *Objectives:* Here we studied the formation, ultrastructure and composition of platelet-derived microparticles from isolated human platelets, either quiescent or stimulated with one of the following activators: arachidonic acid, ADP, collagen, thrombin or calcium ionophore A23187. *Methods:* Using flow cytometry, transmission and scanning electron microscopy, we analyzed the intracellular origin, structural diversity and size distributions of the subcellular particles released from platelets. *Results:* The structure, dimensions and intracellular origin of microparticles depend on the cell-activating stimulus. The main structural groups include a vesicle surrounded by one thin membrane or multivesicular structures. Thrombin, unlike other stimuli, induced formation of microparticles not only from the platelet plasma membrane and cytoplasm but also from intracellular structures. A fraction of these vesicular particles having an intracellular origin contained organelles, such as mitochondria, glycogen granules and vacuoles. The size of platelet-derived microparticles depended on the nature of the cell-activating stimulus. *Conclusion:* The results obtained provide a structural basis for the qualitative differences of various platelet activators, for specific physiological and pathological effects of microparticles, and for development of advanced assays.

Keywords: blood microparticles; cellular microvesicles; electron microscopy; platelet activation; platelets.

Correspondence: John W. Weisel, Department of Cell and Developmental Biology, University of Pennsylvania School of Medicine, 1154 BRB II/III, 421 Curie Blvd, Philadelphia, PA 19104-6058, USA
Tel.: +1 215 898 3573
E-mail: weisel@mail.med.upenn.edu

Received: 22 October 2016
Manuscript handled by: P. H. Reitsma
Final decision: P. H. Reitsma, 5 May 2017

Introduction

Activation and apoptosis of cells, including platelets, are accompanied by formation of extracellular microparticles (MPs) [1]. Generation of MPs is a physiologic mechanism and a pathogenic component in diseases [2–4]. Platelets perform multiple functions, including their important participation in hemostasis and thrombosis and many diverse and important biological properties [5]. Platelet MPs comprise the main fraction of circulating MPs in the blood of healthy subjects and patients [6].

One of the properties of platelet-derived MPs is the accelerating effect on thrombin formation that has been shown to promote thrombotic disorders [7]. Furthermore, platelet-derived MPs are involved in the immune response, inflammation, angiogenesis, regeneration and metastasis [4,8,9]. They can promote healing, act as pro-inflammatory carriers and contribute to tumorigenesis [10,11]. Multiple roles that platelet MPs play in health and disease are a result of their variability in composition

and structure. Because of their pathogenic potential, platelet-derived MPs attracted attention as biomarkers [12,13], but their detection depends on detailed knowledge of their physical and biological properties. In this work, we investigated mostly morphological aspects of formation of platelet-derived MPs in order to develop a systematic structural approach to complement flow cytometry. Our identification and quantification of the multiplicity of types of MPs provides a structural basis for the qualitative difference of various platelet activators, for specific physiological and pathological effects of MPs, for development of advanced assays, and for the potential mechanism of thrombocytopenia associated with thrombosis.

Materials and methods

Isolation and characterization of platelets

Platelets were isolated from healthy donors not taking antiplatelet medications. Blood samples were collected following informed consent under approval by the Ethical Committee of the Kazan Medical Academy (Kazan, Russia). All procedures were carried out in accordance with the approved guidelines. Citrated blood was centrifuged at 200 *g* for 10 min to obtain platelet-rich plasma (PRP). Platelets were isolated from PRP by gel filtration on Sepharose 2B (GE Healthcare, Uppsala, Sweden) equilibrated with Tyrode's buffer (4 mmol L^{-1} HEPES, 135 mmol L^{-1} NaCl, 2.7 mmol L^{-1} KCl, 2.4 mmol L^{-1} $MgCl_2$, 5.6 mmol L^{-1} D-glucose, 3.3 mmol L^{-1} NaH_2PO_4, 0.35 mg mL^{-1} bovine serum albumin, pH 7.4). Platelets were used within 3 h after blood collection. Cell viability was ~97% based on maintenance of the mitochondrial membrane potential ($\Delta\psi_m$) determined by flow cytometry using a $\Delta\psi_m$-sensitive fluorescent dye MitoTracker-DeepRed (Invitrogen, Waltham, MA, USA). In addition, platelets' functionality was assessed using flow cytometry to determine their ability to express P-selectin (CD62p) and active integrin αIIbβ3 (determined by fibrinogen-binding capacity) before and after activation with thrombin-receptor activating peptide (TRAP) (Bachem Americas, Torrance, CA, USA) (Figure S1).

Flow cytometry of platelets and MPs

A total of 200 000 platelets in 150 μL Tyrode's buffer (without or with 2 mmol L^{-1} $CaCl_2$) were incubated at 37 °C in the absence or presence of arachidonic acid, ADP, collagen, thrombin or Ca^{2+}-ionophore A23187. The stimulants were added to platelets in various amounts to determine an MP-producing concentration (Figures S2 and S3). After 15- or 60-min incubation, the samples were treated with FITC-labeled AnnexinV (BioLegend, San Diego, CA, USA) and anti-CD41-PE-labeled antibodies (Life Technologies, Frederick, MD, USA) for 5 min at room temperature in the dark. Then, 350 μL of the Ca^{2+}-containing AnnexinV-binding buffer (10 mmol L^{-1} HEPES, 140 mmol L^{-1} NaCl, 2.5 mmol L^{-1} $CaCl_2$, pH 7.4) was added and in 10 min 30 000 events were collected using a FacsCalibur flow-cytometer (BD Biosciences, San Jose, CA, USA). CD41-positive cells were gated in the platelet-specific dot-plots. The upper limit of the MP quadrant gate in FSC-FL2 dot-plots was established using 1.0-μm beads (ThermoFisherSci, Eugene, OR, USA) and platelets were gated by their binding of anti-CD41-PE-labeled antibodies (CD41-positive MPs) (Figure S4A). The lower limit determined with Fluorescent Nanobeads (Spherotech, Lake Forest, IL, USA) was ~500 nm for the forward-scatter mode and ~220 nm for the side-scatter mode, which is consistent with the literature [13,14]. Therefore, platelet-derived MPs were identified as the events that contained a platelet-specific marker CD41 below the 1-μm size using FSC/FL CD41 dot-plots (Figure S4C,D, quadrant Q2). Platelet MPs that expressed phosphatidylserine were quantified as CD41 positive and AnnexinV positive in dot-plot quadrants using CellQuest Pro and FlowJo software. At least four independently isolated platelet preparations were studied under each experimental condition.

Platelet activation for transmission electron microscopy

Platelets in Tyrode's buffer containing or not containing $CaCl_2$ (10 mmol L^{-1}) were activated by adding 50 μmol L^{-1} arachidonic acid (Sigma-Aldrich, St. Louis, MO, USA), 5 μmol L^{-1} ADP (Chrono-log Corp., Havertown, PA, USA), 5 μg mL^{-1} collagen (Renam, Moscow, Russia), or 1 U mL^{-1} thrombin (Sigma-Aldrich, St. Louis, MO, USA) (final concentrations), followed by incubation at 37 °C for 15 or 60 min. Untreated platelets were incubated for 15 or 60 min at 37 °C before examination and used as a negative control. The final volume of each sample was 560 μL containing ~80 × 10^6 cells mL^{-1}. The 15-min point has been empirically found to be the earliest time during which all of the activators studied have induced a remarkable release of MPs and platelet structural rearrangements. The 60-min time-point was used to ensure that there were no specific time-dependent changes that were not captured at 15 min [15].

Transmission electron microscopy of platelets

Immediately after incubation, the platelet suspension was fixed in 2.5% glutaraldehyde in Tyrode's buffer for 1.5 h at room temperature and then centrifuged at 1500 *g* for 5 min. The precipitate was washed with Tyrode's buffer and then post-fixed with 1% osmium tetroxide in the same buffer with sucrose (25 mg mL^{-1}) for 2 h. The samples were dehydrated in ascending ethanol concentrations, acetone and propylene oxide. The Epoxy-resin medium was Epon 812 (Fluka, Buchs, Switzerland). The samples were allowed to polymerize for 3 days at increasing temperature of 37–60 °C. Ultrathin sections were cut using

ultramicrotome-III (LKB, Bromma, Sweden) and stained with saturated aqueous uranyl acetate (Serva, Heidelberg, Germany) at 60 °C for 10 min and lead citrate (Serva) at room temperature for 10 min. The specimens were examined using an electron microscope JEM-1200EX (JEOL, Tokyo, Japan) at an operating voltage of 80 kV. The ultrastructural changes at each experimental condition studied were based on three independent platelet preparations with at least three samples processed from each cell preparation. Not less than 40–50 ultrathin sections were viewed and analyzed, followed by imaging of at least 150–200 cells at each experimental condition.

Preparation of platelets for scanning electron microscopy

To stimulate MP production, gel-filtered platelets were incubated for 15 min at 37 °C with 1 U mL^{-1} thrombin. After incubation, the platelets were fixed in 2% glutaraldehyde in 50 mmol L^{-1} sodium cacodylate buffer, pH 7.4, containing 100 mmol L^{-1} NaCl, for 30 min at room temperature. Fixed platelets were layered on a carbon filter (0.4-μm pore size) and centrifuged at 150 *g* for 15 min. The samples were rinsed three times with the same buffer for 5 min, dehydrated in ethanol and dried overnight in hexamethyldisilazane (EMS, Hatfield, PA, USA). A thin (≈15 nm) film of gold-palladium was layered on the samples using a sputter coater (Polaron e5100; Quorum Technologies, Laughton, East Sussex, UK). Micrographs were taken with a Quanta FEG250 (FEI, Hillsboro, OR, USA) scanning electron microscope.

Isolation of platelet-derived MPs for transmission electron microscopy

Platelets were isolated as described above. To stimulate MP production, platelets were incubated for 15 min at room temperature with 15 μmol L^{-1} calcium ionophore A23187, 1 U mL^{-1} thrombin or 5 μg mL^{-1} collagen; collagen was applied at 37 °C as well. After incubation, cells were removed by centrifugation at 2000 *g* for 10 min, followed by centrifugation at 7000 *g* for 10 min at room temperature to remove cellular particulate material denser than MPs. The supernatant containing MPs was collected and prepared for electron microscopy. A 150-mesh formvar carbon-coated grid (EMS, USA) was placed on a 20-μL sample drop for 3 min and blotted with a filter paper to remove the excess liquid. The sample was stained by placing the grid on a 20-μL drop of 2% uranyl acetate for 15–20 s followed by blotting and air drying. The specimens were examined in a Jem-1200EX electron microscope (Jeol).

Statistical analysis

Numerical data were analyzed using MS Office Excel (Microsoft Corporation, 2010, Redmond, WA, USA) and GraphPad Prism 5 software (GraphPad Software, Inc, La Jolla, CA, USA). Averages were analyzed for statistical significance using two-tailed unpaired *t*-tests for parametric data or the Mann–Whitney test for the data with non-parametric data arrays.

Results

Formation of platelet-derived MPs assessed by flow cytometry

Flow cytometry demonstrated that after 15 and 60 min of platelet incubation the total number of CD41-positive particles with size smaller than platelets (presumed platelet-derived MPs) was increased under the influence of Ca^{2+}-ionophore A23187 (Fig. 1A). The number of AnnexinV-positive platelet-derived MPs that expressed

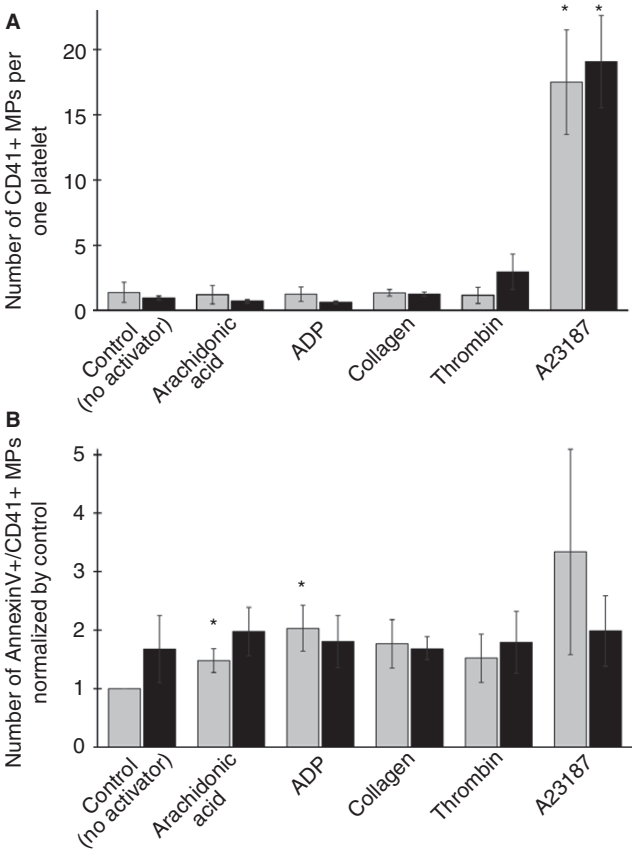

Fig. 1. Flow cytometry of microparticles (MPs) formed after 15 min (light bars) and 60 min (dark bars) incubation of platelets under various experimental conditions. (A) The number of CD41-positive platelet-derived MPs normalized by the number of gated platelets. (B) The number of Annexin V+/CD41+ double-positive MPs formed under various experimental conditions normalized by the number of Annexin V+/CD41+ double-positive MPs formed after 15 min incubation of control untreated platelets. The stimulants were applied at the following concentrations: 50 μmol L^{-1} arachidonic acid, 5 μmol L^{-1} ADP, 1 U mL^{-1} thrombin, 5 μg mL^{-1} collagen, 15 μmol L^{-1} Ca^{2+}-ionophore A23187. The results are presented as a mean ± SEM. *$P < 0.05$.

phosphatidylserine increased significantly in the platelet preparations treated with arachidonic acid and ADP after 15 min of incubation (Fig. 1B). In 60 min the number of MPs was insignificantly different compared with the untreated platelets, probably because of a relatively high level of spontaneous MP release by 'resting' platelets. In the presence of Ca^{2+} the MP production increased with most stimulants (Figure S2B), including AnnexinV-positive and CD41-positive vesicles (Figure S3B); however, Ca^{2+} did not change dramatically the relative MP production by various stimuli. Taken together, the results of flow cytometry demonstrate that preparations of isolated human platelets, either untreated or treated with activators, contain platelet-derived MPs, which were further studied using electron microscopy.

Ultrastructural characterization of resting and activated platelets, the source of MPs

In resting platelets, the average diameter for the round-shaped cell was 2–4 μm and for the elliptical cells it was 3–4 μm along the long axis and 0.8–1.5 μm along the short axis, which corresponds to the reported dimensions [16]. The α-granules, dense granules, lysosomes, peroxisomes, mitochondria and glycogen granules were visualized; the open canalicular system (OCS) was displayed as vacuoles and numerous convoluted tunnels (Figs. 2A, 3A,B and S5A,B). Platelet activation was associated with characteristic morphological changes that depended on the nature of the stimulus. Arachidonic acid or ADP at 15 min (Fig. 2B,C) or 60 min (Figure S5C,D) induced moderate invaginations and protrusions of the plasma membrane and enlargements of the lumen of the OCS with formation of intracellular vacuoles that contained various inclusions, such as α-granules, δ-granules, membrane components and loose-grained inclusions.

The most significant structural changes were observed after incubation of platelets with thrombin (Figs. 2D and 3C–F). The plasma membrane formed deep invaginations and folds, followed by formation of amoeba-like platelets and further breakdown of the platelet bodies into fragments. The cytoplasm of the cells became more electron-dense compared with the untreated cells, and almost did not contain secretory granules. The whole platelet body was penetrated with tortuous and narrow OCS exiting to the cell surface. The fragments of disintegrated platelets were diverse in size and shape and contained various intracellular components, including cellular organelles (Fig. 5D). Similar ultrastructural changes were detected after 15 or 60 min of incubation with thrombin (Figs. 3C,D and S5E). The observed effects of thrombin were Ca^{2+} independent, so that the invaginations of the plasma membrane and fragmentation of cell bodies occurred in the presence of Ca^{2+} as well (Fig. 3E,F).

Formation of platelet MPs

When transmission electron micrographs of platelets were analyzed with special attention to extracellular structures, a substantial number of MPs produced by resting and activated cells were revealed (Table 1). As a result of platelet activation with arachidonic acid or ADP after 15 min of incubation, a significant increase of the number of MPs was observed (2.7- and 2.5-fold, respectively), compared with untreated platelets. The average number of MPs per 100 cells continued to grow and after 60 min of incubation increased by about 2-fold for arachidonic acid and ADP compared with 15 min. The biggest increase of MP formation was observed in control untreated platelets, in which the number of MPs at 60 min rose almost 4-fold compared with the 15-min time-point, suggesting a marked spontaneous release of MPs over time.

Most MPs formed spontaneously or induced by the activators were located on or near the plasma membrane, forming blebs and knobs that were likely to be captured in the process of being released into the extracellular space. MPs that are seemingly at various stages of formation and peeling from the platelet surface can be used to piece together a plausible sequence of events (Fig. 4A). An early step is protrusion of the plasma membrane; then the contact area between the MP and platelet body is reduced, and the edges of the convex membrane merge and get constricted, thus leading to formation of a spherical bubble. Finally, new MPs get separated and released from the platelet body (Fig. 4B). Similarly, nascent MPs were visualized on the tip of a pseudopod formed as a result of progressive protrusion of the plasma membrane (Fig. 4D). Of course, without Z-plane images we may only surmise a sequence of events based on the overall logic of the MP formation process.

Under various conditions of platelet activation MPs were produced not only from the surface of the platelet body or from pseudopods, but also from the OCS. Figure 4(C) shows formation and release of an MP into the extracellular space from a canal of the OCS. When platelets were treated with thrombin, proliferation of the canals of the OCS along with rearrangement of the cytoskeleton led to deep invaginations of the plasma membrane and fragmentation of the cytoplasm, followed by disintegration of the platelet (Figs. 2D, 3C–F, 4D and 5D).

Consistent with the data obtained by transmission electron microscopy, the results of scanning electron microscopy demonstrated that control platelets had a discoid shape (Fig. 4E), whereas activated platelets aggregated and underwent dramatic morphological changes, such as loss of the discoid shape and formation of pseudopodia. Most importantly, activated platelets displayed knobs and blebs on their surface, confirming production of MPs from the plasma membrane (Fig. 4F).

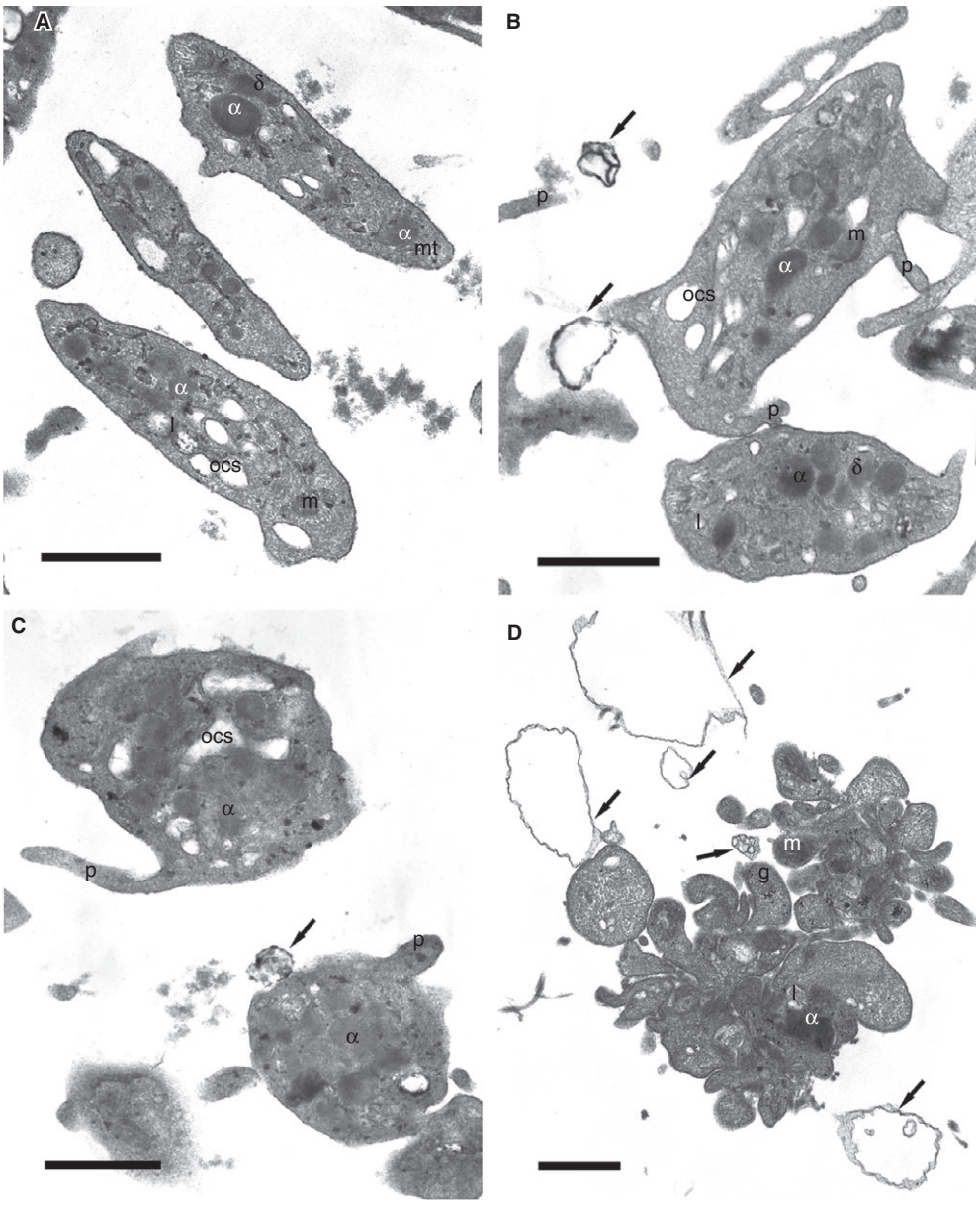

Fig. 2. Representative transmission electron micrographs of control untreated platelets (A) and platelets incubated with 50 μmol L^{-1} arachidonic acid (B), 5 μmol L^{-1} ADP (C) and 1 U mL^{-1} thrombin (D) for 15 min at 37 °C. The designated structures are α-granules (α), δ-granules (δ), glycogen granules (g), lysosome (l), mitochondria (m), microtubules (mt), open canalicular system (ocs) and pseudopod (p). The arrows indicate microparticles (MPs). Magnification bars = 1 μm.

Structural heterogeneity of platelet MPs

Platelet-derived MPs released spontaneously or after activation turned out to be quite heterogeneous in structure. Altogether they could be segregated into the following groups: (i) electron-transparent MPs with contents confined with a single membrane, (ii) multivesicular MPs (i.e. large vesicles containing multiple smaller vesicles inside); and (iii) electron-dense MPs containing various organelles (Fig. 5). We observed formation of all these types of MPs in activated platelets, but control untreated platelets did not form type 3 MPs. The most common MPs had a single membrane and were electron transparent. These MPs originated from the plasma membrane and had the greatest variation in size, ranging from 0.2 μm (Fig. 4B) to 2 μm (Fig. 2D). Multivesicular particles were composed of several small vesicles inside a common membrane or without any visible membrane, perhaps as a result of aggregation of the smaller vesicles. The internal microvesicles could be located close to each other or loosely packed, if they were within a larger vesicle (Figs. 3C and 5B,C). The multivesicular MPs could contain up to 10–15 individual vesicles. The most remarkable heterogeneity was observed in thrombin-activated

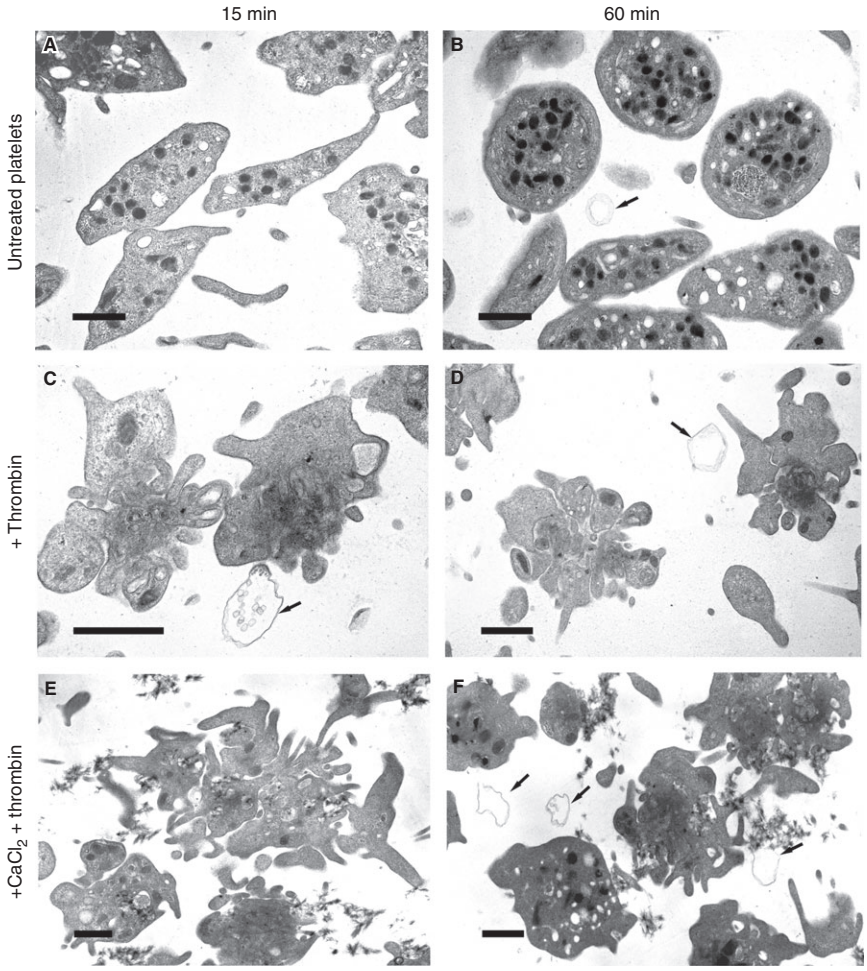

Fig. 3. Representative transmission electron micrographs of control untreated platelets (A, B), platelets incubated with 1 U mL^{-1} thrombin alone (C, D) and 1 U mL^{-1} thrombin in the presence of 10 mmol L^{-1} $CaCl_2$ (E, F) for 15 min (A, C, E) and 60 min (B, D, F) at 37 °C. The arrows point at microparticles (MPs). Magnification bars = 1 μm.

platelets that formed all of the structural variants of MPs (Figs. 2D, 3C,D and 5D). After stimulation by thrombin, the cellular fragments were confined by the plasma membrane and contained cytoplasm, including various cellular components and organelles. Figure 5(D) shows platelet fragments containing a mitochondrion, and α-granule or glycogen granules.

Dimensions of platelet-derived MPs

In the electron micrographs of platelet preparations we observed MPs between 50 and 2000 nm in size but the vast majority (typically > 80%) were within the 50–500 nm range. The size of MPs did not depend on their structural organization and whether they originated from the plasma membrane or intracellular structures. MPs confined within a single membrane might be as large as 1500–2000 nm, whereas some of them were much smaller (700–1000 nm). We detected very small vesicular particles (50–70 nm) inside a large particle (Fig. 5B). The electron-

Table 1 Number of microparticles (MPs) produced by untreated and activated platelets

	No. of MPs/100 platelets	
Activator	15 min	60 min
Control (no activator)†	8.8 ± 2.6 (*n** = 300)	34.3 ± 2.4 (*n* = 200)
Arachidonic acid (50 μmol L^{-1})†	23.9 ± 0.6 (*n* = 300)	44.3 ± 4.5 (*n* = 200)
ADP (5 μmol L^{-1})†	21.9 ± 4.7 (*n* = 300)	42.9 ± 4.8 (*n* = 200)
Thrombin (1 U mL^{-1})‡	–	–

**n* values represent the number of cells analyzed in the micrographs at a relatively low magnification of 8000–10 000×. †All the averages (mean ± SD) are significantly different compared with the corresponding control (within the columns) and between 15 and 60 min of incubation (within the rows); the MP-producing activities of various triggers (within the columns) are incomparable because the effects are dose dependent (see Figs S2 and S3). ‡Quantification of MPs per number of platelets in thrombin-treated platelets was impossible because most platelet bodies fell apart into organelle-containing particles.

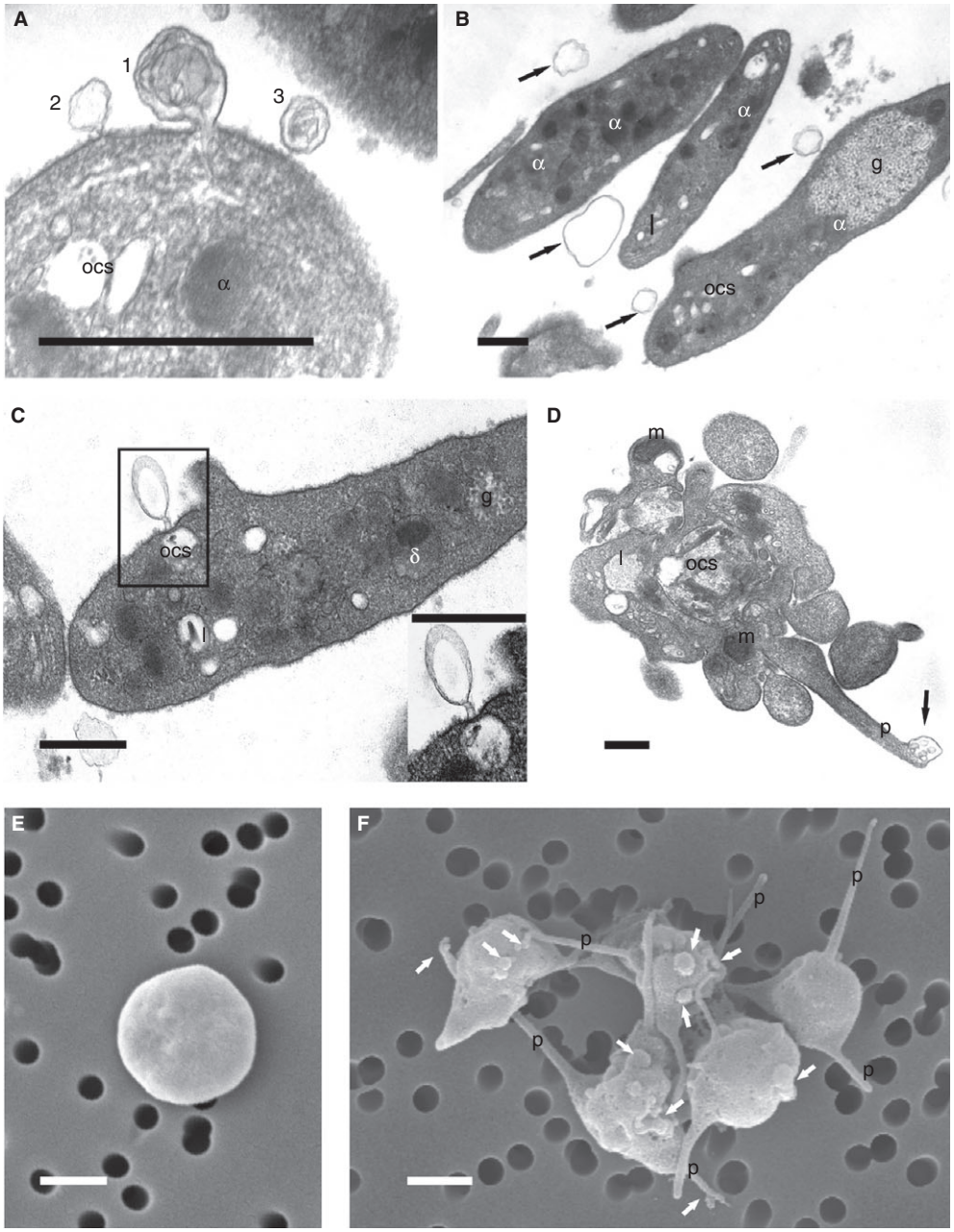

Fig. 4. Transmission (A–D) and scanning (E, F) electron micrographs showing formation of platelet microparticles (MPs) from various parts of a cell. (A) Budding of MPs from the outer plasma membrane (1, 2, 3 – MPs at various stages of formation). (B) Separated MPs in the extracellular space (shown by arrows). (C) Formation of an MP connected to the OCS. (D) Formation of an MP (arrow) at the end of a pseudopod. (E) A resting platelet. (F) An aggregate of thrombin-activated platelets with MPs budding from their plasma membrane (shown by arrows). Magnification bars = 0.5 μm (A–D) and = 1 μm (E, F).

dense particles originating from disintegration of the platelet body (Figs. 2D, 3C,D and 5D) were within 100–1000 nm, which is the canonical size range for platelet-derived MPs [17].

Transmission electron microscopy of isolated MPs was used to analyze the morphology and size of several hundred platelet-derived MPs (Fig. 6). MPs generated by non-activated platelets were all circular and smooth (Fig. 6A). MPs from platelets activated with Ca^{2+}-ionophore and collagen also had a circular shape but were more heterogeneous (Fig. 6B,D). The MPs from thrombin-activated platelets were relatively small (50–100 nm) and were either spherical or elongated with a rough surface and thin offshoots (Fig. 6C).

The size distributions of platelet-derived MPs are shown in Fig. 7. MPs from the quiescent platelets varied within 30–500 nm in size, with a major peak at 71 ± 36 nm and a shoulder peaking at 168 ± 72 nm (Fig. 7A). Asymmetry of the histogram towards the higher numbers indicates the presence of a fraction of

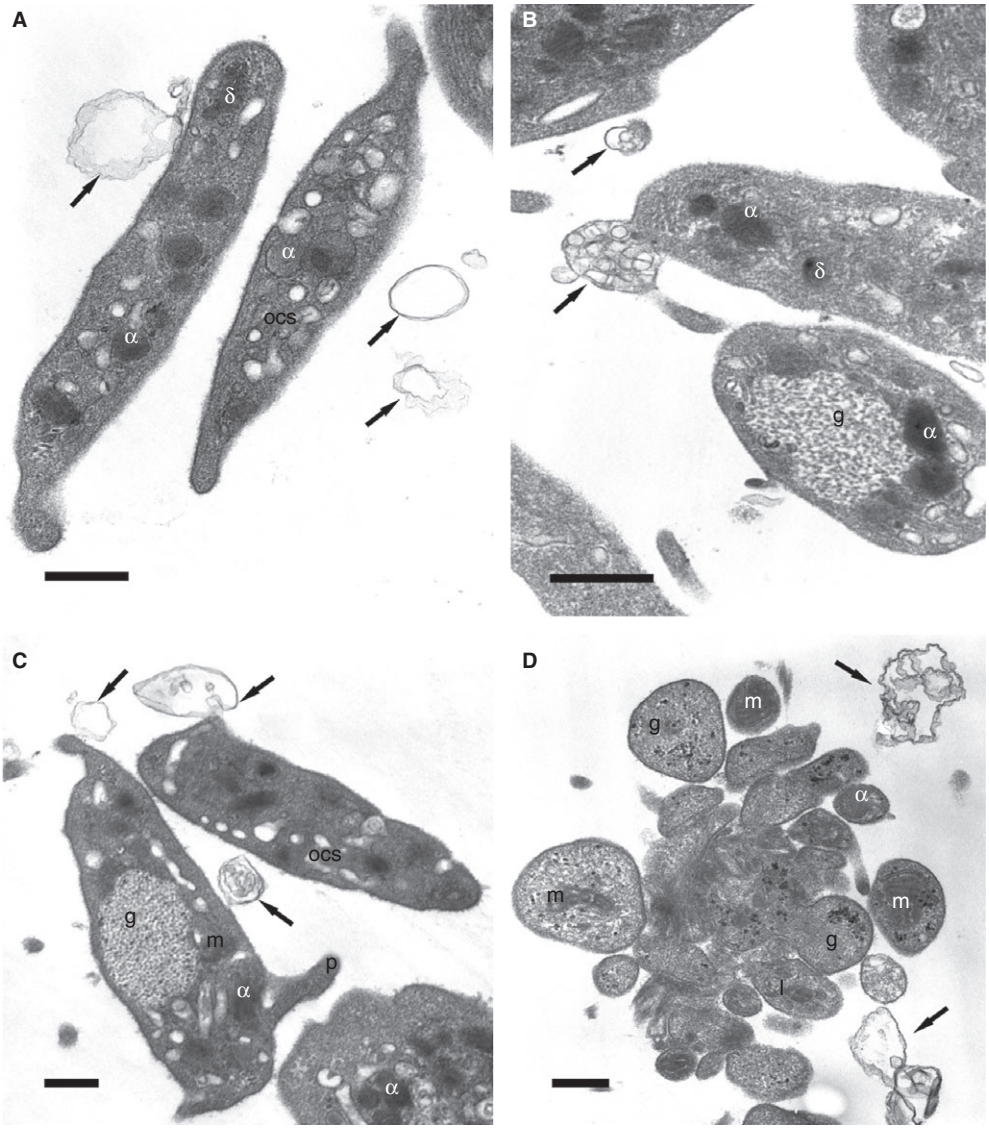

Fig. 5. Transmission electron micrographs demonstrating structural variability of platelet-derived microparticles (MPs). (A) MPs with a single membrane. (B) Multivesicular MPs. (C) MPs of various morphological structures. (D) MP-like structures formed during thrombin-induced fragmentation of a platelet. Arrows indicate MPs. Magnification bars = 0.5 μm.

MPs that were 150–200 nm and more in diameter. MPs from platelets activated with Ca^{2+}-ionophore were highly heterogeneous and displayed three peaks at 76 ± 26 nm, 199 ± 38 nm and 312 ± 32 nm (Fig. 7B), reflecting an increase of the fraction of large MPs that were not seen in the resting platelets. Collagen induced formation of an even more heterogeneous population of MPs in a broad range of sizes with peaks at 73 ± 44 nm, 199 ± 38 nm and 312 ± 106 nm (Fig. 7C). By contrast, activation of platelets with thrombin was accompanied by an increase of the fraction of small particles peaking at 72 ± 40 nm (Fig. 7D), which presumably comprise exosomes as opposed to the larger particles, which are likely to represent ectosomes [18]. The exosomes and ectosomes are two main types of extracellular vesicles that are distinct by the mechanism of formation and their size. The ectosomes are the MPs that are formed from the plasma membrane and have a size within 0.1–1 μm and the exosomes originate from intracellular membranous structures and have a size of 50–100 nm [19].

It is noteworthy that the histograms presented in Fig. 7 do not include MPs larger than 500 nm, whereas in the platelet preparations, we observed MPs up to 1000–1500 nm in size. This difference could be potentially attributed to a methodological issue, namely, the larger MPs might be removed during centrifugation at 7000 *g*. To test this possibility, we analyzed the composition of the precipitate after centrifugation at 7000 *g* (Figure S6A), which turned out to contain very small relatively homogeneous particles ≈120 nm in size. The supernatant contained significantly larger particles that were heterogeneous in size

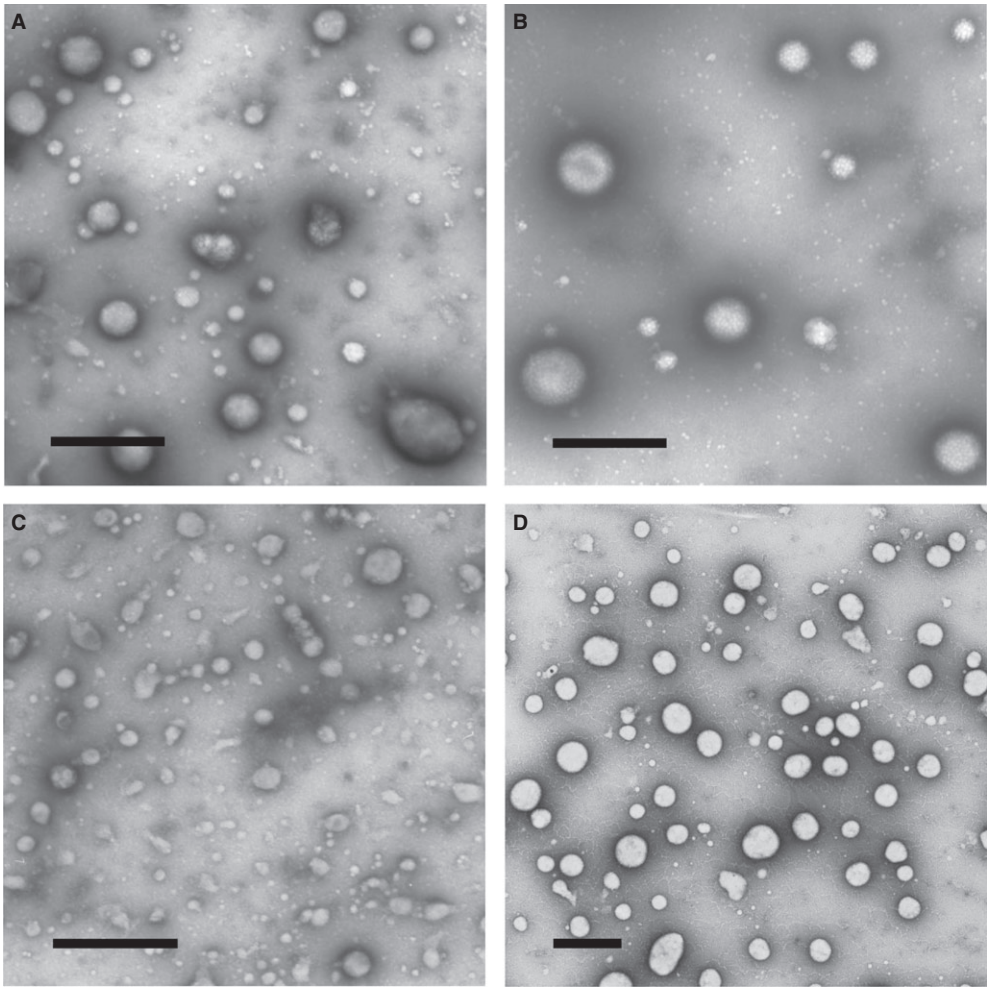

Fig. 6. Transmission electron micrographs of negatively stained isolated platelet-derived microparticles (MPs). MPs isolated from a preparation of untreated platelets (A); MPs isolated from a preparation of platelets activated with 15 μmol L^{-1} Ca^{2+}-ionophore A23187 (B), 1 U mL^{-1} thrombin (C) and 5 μg mL^{-1} collagen (D). Magnification bars = 0.5 μm.

(Figure S6B) and presumably had a low physical density (consistency) that made them float rather than settle. Therefore, the centrifugation did not remove larger MPs but, instead, eliminated the fraction of heavy small homogeneous particles, probably comprising secretory δ-granules that have a size of about 150 nm [16].

To compare the structure of circulating MPs with those formed *in vitro*, we analyzed the morphology of MPs isolated from plasma of a healthy donor and patients with diseases associated with activation of platelets as well as other blood cells and endothelium (Figure S8). The size distribution of MPs from normal plasma was in general agreement with MPs from resting platelets (Fig. 7A). The size distribution of MPs isolated from the plasma of patients with (pro)thrombotic conditions (disseminated intravascular coagulation, heparin-induced thrombocytopenia and systemic lupus erythematosus) was consistently shifted towards the higher dimensions, suggesting that 'pathological' MPs are distinct from 'normal' MPs.

Discussion

Although flow cytometry confirmed the ability of platelets to form MPs, this method generally does not detect particles smaller than 300–400 nm [13,14] that comprise a substantial portion of MPs. In addition, flow cytometry does not provide information on the structure of MPs [17,20,21], which can be gleaned only from electron microscopy. The latter was used here to study the intracellular origin of platelet MPs and their structural diversity. Variants of electron microscopy have been used to study the ultrastructure of MPs, including cryo-electron microscopy, as well as negative staining or immuno-gold labeling techniques [2,20,22]. In this work, we used a combination of transmission and scanning electron microscopy to characterize platelet-derived MPs with respect to the structure of resting and differentially activated cells.

Even untreated platelets produce MPs (Figs. 3B, 4B and S5A,B), for which there are two mutually non-exclusive explanations. First, isolated platelets are inevitably

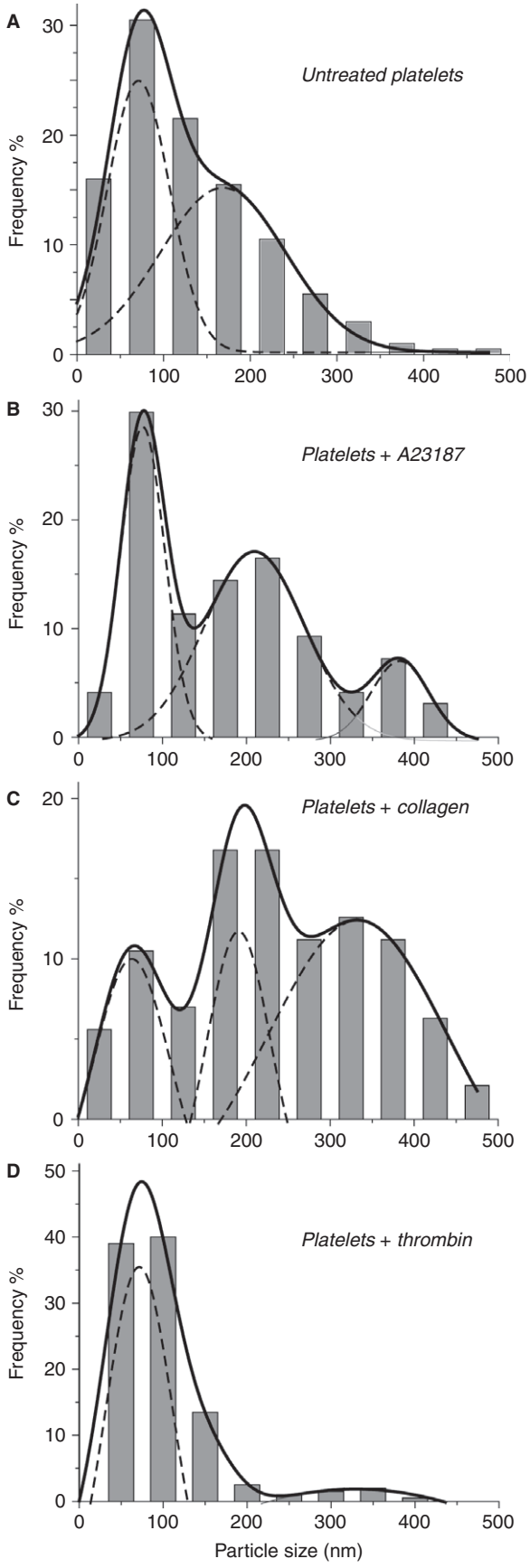

Fig. 7. Size distributions of microparticles (MPs) isolated from untreated platelets (A) and platelets activated with 15 μmol L^{-1} Ca^{2+}-ionophore (B), 5 μg mL^{-1} collagen (C) and 1 U mL^{-1} thrombin (D). Dimensions were determined with ImageJ using electron micrographs of isolated negatively stained MPs. The total number of MPs in each group (n = 200) is taken as 100%.

exposed to physical and chemical influences that can activate the cells. Alternatively, the process of MP formation may be a function of cells in conditions of physiological quiescence [23]. Platelet-derived MPs circulating in the blood of healthy subjects are abundant enough to have significant effects on formation and properties of fibrin clots [24].

To mimic physiological activation and enhance MP production, platelets were treated with various stimuli. In agreement with the literature [25–27], we observed a classical subcellular organization of resting platelets and well-known morphological signs of their activation (Fig. 2B–D). Notably, the effects of arachidonic acid and ADP were relatively mild and similar to each other (Fig. 2B,C), whereas thrombin, a strong platelet activator, caused profound structural rearrangements of the cells right up to their breakdown (Figs. 2D, 3C,D, 5D and S5E). This finding suggests that thrombin-induced fragmentation of platelets may be a mechanism for apoptotic [21] or non-apoptotic cell death, resulting in elimination of activated platelets from the blood. So far, the reduced platelet counts in thrombotic states, such as disseminated intravascular coagulation [28], heparin-induced thrombocytopenia [29] or thrombotic thrombocytopenic purpura [30], have been related mainly to platelet consumption. Therefore, platelet disintegration induced by thrombin may be an under-appreciated mechanism for thrombocytopenia associated with thrombosis.

By their intracellular origin, cell-derived MPs are usually segregated into ectosomes from the outer cell membrane [31] and exosomes from internal membranous structures [32,33]. The exosomes are generally smaller than ectosomes (50–100 nm vs. 100–1000 nm, respectively). We found that most frequently MPs were formed from the plasma membrane (Figs. 4A and 5A,C); alternatively, we observed formation of MPs primarily derived from intracellular structures (Fig. 4C). Moreover, in histograms we observed relatively distinct fractions of MPs 50–100 nm and > 200 nm in size (Figs. 7 and S7). Thus, our study confirms that this classification is applicable to platelet-derived MPs.

With various platelet stimulants we have identified a number of structural variants of MPs that allowed segregating them into three main groups, namely individual single-layered, multivesicular structures and membrane-confined particles with organelles inside (Fig. 5). The latter structures, in addition to cytosol, could contain mitochondria, cytoskeletal elements, glycogen granules

and small vacuoles. MPs have been shown to serve as carriers of various bioactive molecules, to convey them to other cells and impart new biological properties to them [9]. Our study as well, as others [1], has demonstrated the ability of platelet MPs to carry encapsulated cellular organelles, which provides a basis for the intercellular exchange of mitochondria or mitochondrial DNA, which has great functional consequences [34].

There are few morphological studies on cellular MPs that, in addition to commonly observed 'bubbles', describe a variety of MP-like structures. Electron microscopy showed that some pseudopodia of activated platelets contained terminal complex multivesicular structures of an unknown nature [35]. Another study [36] described MPs obtained from the supernatant of washed platelets after stimulation by thrombin. These MPs had heterogeneous structures of varying size, shape and density; some of them had multilamellar membranes and contained dense membrane-enclosed granules as well as other structures resembling mitochondria. Our results are consistent with the published data on the structural heterogeneity of platelet MPs. However, unlike the earlier publications, our work defines their intracellular origin, extends the morphological variability of platelet-derived MPs and provides detailed structural characteristics of various types of MPs produced by resting and activated platelets. Importantly, our results support a notion regarding the qualitative difference and specificity of each platelet stimulant, leading to production of multifunctional MPs with various structures and compositions. We have confirmed and complemented earlier data showing that various platelet stimulants induce formation of MPs with distinct phospholipid [37] and protein [38,39] composition that underlies their role as intercellular transmitters of biological information [40].

Platelet MPs have been shown to be very diverse in size, varying from 0.1 μm [41] to 1 μm [20]. Our results are generally consistent with the published dimensions of MPs, but with an important addition, namely that the size of platelet MPs depends mainly on the nature of the activating stimulus and the intracellular origin. For example, the MPs from Ca^{2+}-ionophore-activated platelets are larger and represent ectosomes, whereas MPs from thrombin-activated platelets had a substantial population of small and very small particles comprising exosomes. The size of MPs is critically important for the development of new reliable and sensitive assays for MPs, which are necessary to help alleviate the confusion in this field.

In conclusion, our study has shown structural heterogeneity of platelet-derived MPs and established a link between the nature of cell-activating stimuli, MP morphology and the intracellular source of their formation. We propose the morphological classification of platelet MPs based on their detailed structure, dimensions and mechanisms, the intracellular sources of their formation, and the presence of inclusions and organelles inside MPs. Specifically, we have characterized three main structural groups of MPs: (i) MPs surrounded by one thin membrane, (ii) MPs with multivesicular structure, and (iii) MPs containing cellular organelles. The results obtained are important for understanding the multiplicity of types of MPs and provide a structural basis for the qualitative difference of various platelet activators, for specific physiological and pathological effects of MPs and for development of advanced assays.

Addendum

J. W. Weisel, R. I. Litvinov, and L. Rauova designed the research; A. A. Ponomareva, T. A. Nevzorova, E. R. Mordakhanova, and I. A. Aandrianova performed experiments; A. A. Ponomareva, T. A. Nevzorova, I. A. Aandrianova, R. I. Litvinov, L. Rauova, and J. W. Weisel analyzed data; A. A. Ponomareva, T. A. Nevzorova, R. I. Litvinov, L. Rauova, and J. W. Weisel wrote the paper. All authors reviewed the results and approved the final version of the manuscript.

Acknowledgements

The authors thank L. Zubairova for helpful suggestions. The work is supported by NIH grants UO1 HL116330, HL090774 and P01 HL110860 and the Program for Competitive Growth at Kazan Federal University.

Disclosure of Conflict of Interests

The authors state that they have no conflict of interest.

Supporting Information

Additional Supporting Information may be found in the online version of this article:

Fig. S1. Functionality of isolated platelets was assessed by the ability to express P-selectin and active integrin αIIbβ3 in response to stimulation.
Fig. S2. Flow cytometry data showing the number of CD41-positive microparticles (MPs) normalized by the number of gated platelets after 15 min incubation of platelets in the absence and presence of various amounts of activators without (A) or with (B) 2 mmol L^{-1} $CaCl_2$.
Fig. S3. The number of Annexin V+/CD41+ double-positive MPs formed after 15 min incubation of platelets in the absence and presence of various amounts of activators without (A) or with (B) 2 mmol L^{-1} $CaCl_2$.
Fig. S4. Flow cytometry of platelets and platelet-derived MPs.
Fig. S5. Representative transmission electron micrographs of untreated platelets and platelets activated by arachidonic acid, ADP and thrombin for 60 min at 37 °C.

Fig. S6. Negatively stained granular structures isolated from a platelet preparation treated with ADP.

Fig. S7. Size distributions of microparticles (MPs) isolated from platelets activated with collagen at room temperature and 37 °C.

Fig. S8. Size distributions of microparticles (MPs) isolated from the plasma of a healthy subject and the plasma of patients with documented disseminated intravascular coagulation (DIC), heparin-induced thrombocytopenia (HIT) and systemic lupus erythematosus (SLE).

References

1 Boudreau LH, Duchez A-C, Cloutier N, Soulet D, Martin N, Bollinger J, Par′e A, Rousseau M, Naika GS, L′evesque T, Laflamme C, Marcoux G, Lambeau G, Farndale RW, Pouliot M, Hamzeh-Cognasse H, Cognasse F, Garraud O, Nigrovic PA, Guderley H, *et al*. Platelets release mitochondria serving as substrate for bactericidal group IIA-secreted phospholipase A2 to promote inflammation. *Blood* 2014; **14**: 2173–83.

2 Kelton JG. The pathophysiology of heparin-induced thrombocytopenia. Biological basis for treatment. *Chest* 2005; **127**: 9–20.

3 Nomura S, Ozaki Y, Ikeda Y. Function and role of microparticles in various clinical settings. *Thromb Res* 2008; **123**: 8–23.

4 Varon D, Shai E. Platelets and their microparticles as key players in pathophysiological responses. *J Thromb Haemost* 2015; **13**: 40–6.

5 Aatonen M, Grönholm M, Siljander PR. Platelet-derived microvesicles: multitalented participants in intercellular communication. *Semin Thromb Hemost* 2012; **38**: 102–13.

6 Horstman LL, Ahn YS. Platelet microparticles: a wide-angle perspective. *Crit Rev Oncol Hematol* 1999; **30**: 111–42.

7 Nomura S, Shimizu M. Clinical significance of procoagulant microparticles. *J Intensive Care* 2015; **3**: 1–11.

8 Thushara RM, Hemshekhar M, Basappa , Kemparaju K, Rangappa KS, Girish KS. Biologicals, platelet apoptosis and human diseases: an outlook. *Crit Rev Oncol Hematol* 2015; **93**: 149–58.

9 Burnouf T, Goubran HA, Chou M-L, Devos D, Radosevic M. Platelet microparticles: detection and assessment of their paradoxical functional roles in disease and regenerative medicine. *Blood Rev* 2014; **28**: 155–66.

10 van der Pol E, Böing AN, Harrison P, Sturk A, Nieuwland R. Classification functions, and clinical relevance of extracellular vesicles. *Pharmacol Rev* 2012; **64**: 677–705.

11 Mezouar S, Mege D, Darbousset R, Farge D, Debourdeau P, Dignat-George F, Panicot-Dubois L, Dubois C. Involvement of platelet-derived microparticles in tumor progression and thrombosis. *Sem Oncol* 2014; **41**: 346–58.

12 Owens AP, Mackman N. Microparticles in hemostasis and thrombosis. *Circ Res* 2011; **108**: 1284–97.

13 Ayers L, Harrison P, Kohler M, Ferry B. Procoagulant and platelet-derived microvesicle absolute counts determined by flow cytometry correlates with a measurement of their functional capacity. *J Extracell Vesicles* 2014; **3**: 25348.

14 Nieuwland R, van der Pol E, Gardiner C, Sturk A. Platelet-Derived Microparticles. In: Michelson AD, ed. *Platelets*, 3rd edn. San Diego, CA, USA: Academic Press, 2013: 453–67.

15 Aatonen MT, Öhman T, Nyman TA, Laitinen S, Grönholm M, Siljander PR-M. Isolation and characterization of platelet-derived extracellular vesicles. *J Extracell Vesicles* 2014; **3**: 24692.

16 Gremmel T, Frelinger AL, Michelson AD. Platelet physiology. *Semin Thromb Hemost* 2016; **42**: 191–204.

17 Lacroix R, Robert S, Poncelet P, Kasthuri RS, Key NS, Dignat-George F. Standardization of platelet-derived microparticle enumeration by flow cytometry with calibrated beads: results of the International Society on Thrombosis and Haemostasis SSC Collaborative workshop. *J Thromb Haemost* 2010; **8**: 2571–4.

18 Cocucci E, Meldolesi J. Ectosomes and exosomes: shedding the confusion between extracellular vesicles. *Trends Cell Biol* 2015; **25**: 364–72.

19 van der Pol E, Hoekstra AG, Sturk A, Otto C, Van Leeuwen TG, Nleuwland R. Optical and non-optical methods for detection and characterization of microparticles and exosomes. *J Thromb Haemost* 2012; **8**: 2596–607.

20 Heijnen HFG., Schiel AE, Fijnheer R, Geuze HJ, Sixma JJ. Exocytosis of multivesicular bodies and α-granules microvesicles by surface shedding and exosomes derived from activated platelets release two types of membrane vesicles. *Blood* 1999; **94**: 3791–9.

21 Leytin V, Allen DJ, Mykhaylov S, Lyubimov E, Freedman J. Thrombin-triggered platelet apoptosis. *J Thromb Haemost* 2006; **4**: 2656–63.

22 Arraud N, Linares R, Tan S, Gounou C, Pasquet J-M, Mornet S, Brisson AR. Extracellular vesicles from blood plasma: determination of their morphology, size, phenotype and concentration. *J Thromb Haemost* 2014; **12**: 614–27.

23 Thushara RM, Hemshekhar M, Kemparaju K, Rangappa KS, Devaraja S, Girish KS. Therapeutic drug-induced platelet apoptosis: an overlooked issue in pharmacotoxicology. *Arch Toxicol* 2014; **88**: 185–98.

24 Zubairova LD, Nabiullina RM, Nagaswami C, Zuev YF, Mustafin IG, Litvinov RI, Weisel JW. Circulating microparticles alter formation, structure, and properties of fibrin clots. *Sci Rep* 2015; **5**: 176110.

25 James G, White MD. Exocytosis of secretory organelles from blood platelets incubated with cationic polypeptides. *Am J Pathol* 1972; **69**: 41–54.

26 Zucker WH, Shermer RW, Mason RG. Ultrastructural comparison of human platelets separated from blood by various means. *Am J Pathol* 1974; **77**: 255–68.

27 Neumüller J, Meisslitzer-Ruppitscha C, Ellinger A, Pavelkaa M, Jungbauer C, Renzb R, Leitner G, Wagner T. Monitoring of platelet activation in platelet concentrates using transmission electron microscopy. *Transfus Med Hemother* 2013; **40**: 101–7.

28 Boral BM, Williams DJ, Boral LI. Disseminated intravascular coagulation. *Am J Clin Pathol* 2016; **146**: 670–80.

29 Cines DB, McMillan R. Pathogenesis of chronic immune thrombocytopenic purpura. *Curr Opin Hematol* 2007; **14**: 511–4.

30 Shatzel JJ, Taylor JA. Syndromes of thrombotic microangiopathy. *Med Clin North Am* 2017; **101**: 395–415.

31 Stein JM, Luzio JP. Ectocytosis caused by sublytic autologous complement attack on human neutrophils. The sorting of endogenous plasma-membrane proteins and lipids into shed vesicles. *Biochem J* 1991; **274**: 381–6.

32 Johnstone RM, Adam M, Hammond JR, Orr L, Turbide C. Vesicle formation during reticulocyte maturation. Association of plasma membrane activities with released vesicles (exosomes). *J Biol Chem* 1987; **262**: 9412–20.

33 Akers JC, Gonda D, Kim R, Carter BS, Chen CC. Biogenesis of extracellular vesicles (EV): exosomes, microvesicles, retrovirus-like vesicles, and apoptotic bodies. *J Neurooncol* 2013; **113**: 1–11.

34 Spees JL, Olson SD, Whitney MJ, Prockop DJ. Mitochondrial transfer between cells can rescue aerobic respiration. *Proc Natl Acad Sci USA* 2006; **103**: 1283–8.

35 Polasek J. The appearance of multivesicular structures during platelet activation as observed by scanning electron microscopy. *Thromb Res* 1982; **28**: 433–7.

36 George JN, Thoi LL, McManus LM, Reimann TA. Isolation of human platelet membrane microparticles from plasma and serum. *Blood* 1982; **60**: 834–40.

37 Biró E, Akkerman JW, Hoek FJ, Gorter G, Pronk LM, Sturk A, Nieuwland R. The phospholipid composition and cholesterol content of platelet-derived microparticles: a comparison with platelet membrane fractions. *J Thromb Haemost* 2005; **3**: 2754–63.
38 Shai E, Rosa I, Parguiña AF, Motahedeh S, Varon D, García Á. Comparative analysis of platelet-derived microparticles reveals differences in their amount and proteome depending on the platelet stimulus. *J Proteomics* 2012; **5**: 287–96.
39 Milioli M, Ibáñez-Vea M, Sidoli S, Palmisano G, Careri M, Larsen MR. Quantitative proteomics analysis of platelet-derived microparticles reveals distinct protein signatures when stimulated by different physiological agonists. *J Proteomics* 2015; **21**: 56–66.
40 Hoyer DP, Korkmaz Y, Grönke S, Addicks K, Wettschureck N, Offermanns S, Reuter H. Differential expression of protein kinase C isoforms in coronary arteries of diabetic mice lacking the G-protein Gα11. *Cardiovasc Diabetol* 2010; **9**: 93.
41 Hughes M, Hayward CPM, Warkentin TE, Horsewood P, Chorneyko KA., Kelton JG. Morphological analysis of microparticle generation in heparin-induced thrombocytopenia. *Blood* 2000; **96**: 188–94.